

Enhancing The Surface Uniformity of Polygon Holes Polishing in Abrasive Flow Machining

Kuan-Yu Chen^{1,a}, K.C. Cheng^{1,b}, A.C. Wang^{2,c}, Y.C. Lin^{3,d}, S.H. Chou^{2,e}

¹ Department of Mechanical Engineering, Chung Yuan Christian University,
200, Chung Pei Rd., Chung Li, Taoyuan County, 32023 Taiwan, R.O.C.

² Department of Mechanical Engineering, Ching Yun University,
229, Jiansing Rd., Chung Li, Taoyuan County, 320 Taiwan, R.O.C.

³ Mechanical Engineering, Nankai University of Technology,
568, Zhongzheng Rd., Caotun, Nantou County 54243, Taiwan, R.O.C.

^agychen@cycu.edu.tw, ^bkccheng20@gmail.com, ^cacwang@cyu.edu.tw, ^dycline@nkut.edu.tw, ^eshchou@cyu.edu.tw

Abstract - The characteristic of Abrasive flow machining (AFM) is a suitable method for complex holes and curved surface machining. However, the conventional AFM methods have difficulty to achieve uniform roughness of radial distribution in polygon holes polishing, due to the radial distance of polygon holes is not symmetry and the abrasive forces are non-uni form in the corner edges. Therefore, abrasive machining of gels with helical passageways are proposed to perform multiple flowing paths of abrasive media, whose flowing behaviour enhances polishing effectiveness by increasing the abrasive surface area and radial shear forces. In this research, an analysis model has been developed in order to understand the motion behaviour of the abrasive medium in the different passageways by utilizing CFD-ACE⁺ software. Finally, numerical results reveal that the percentage change of radial strain-rate deviation can reduce from 72% to 40% for square polygon. Similarly, the improvement rate of helical passageway in hexagon shape is obtained approximately 15% and only nearly 6% improvement percentage for octagon shape. Moreover, in order to verify simulation accuracy, a series of AFM-related experiments pick up ten positions in a radial surface of cross section to test the surface roughness. The experimental results indicate that average improvement percentage of helical passageway in different polygons AFM are all nearly 7% , and surface roughness is more uniform when four helices core is utilized as finishing passageway. Therefore, helical passageway indeed produce multiple flow motion of abrasive medium in AFM and create notable efficiency on good surface roughness and uniformity in radial distributions for polishing polygon holes.

Keywords - Abrasive flow machining (AFM), Helical passageway, Polygon holes, Surface roughness.

I. INTRODUCTION

Generally, the Wire electrical discharge machining (WEDM) is gaining wide acceptance for cutting out the holes of metal components used in the punching or injection molds. However, the parts surfaces are full of micro cracks and craters due to WEDM side effect of subsequent heat erosion, and these defects lead to bad quality of the products surface. Therefore, many approaches have been developed to reduce the surface roughness and increase the machining

precision of parts surface. Those non-traditional processes, such as ultrasonic lapping, electro-chemical polishing, magnetic abrasive finishing and ball burnish machining were being used to meet industries demands [1–4]. Anyway, above methods may exist such as drawback either increased cost due to prolonged machining or limited the shapes to process.

Thus, a kind of simple, low-cost and high effective polishing methods was developed. In AFM, it is an effective means of deburring, finishing and removing recasting layers by flowing of abrasive medium over parts surfaces. The polishing efficiency of AFM had been analyzed using machining parameters and rheological properties of the abrasive media. There are many papers had been published to demonstrate the effectiveness of material removal and surface roughness by modifying some parameters during AFM, such as a high number of machining cycles, high extrusion pressure, high abrasive concentration, low abrasive grain size, a high viscosity of media,...etc [5-8]. While most research had been purely numerical analysis or experimental method, few studies had predicted the polishing results via tests and simulations during AFM. For example, the material removal rate and surface roughness were estimated using the finite element method [9-10]. The active grain density on a medium's surface was also determined by stochastic simulation [11]. This method could be easily extended to simulate the surface generation during AFM.

Recently, a non-Newtonian flow was employed to establish the material properties of abrasive medium by power law equation. The CFD-ACE⁺ software was applied to simulate the flowing motion of abrasive medium in AFM, and to analyze the polishing effects of different abrasive media in a chain hole finishing process [12-14]. In those investigations, a new concept with inserting the mold core into a machining hole to change the passageway shape was developed. The analysis results showed that the distribution of strain rates and shear forces were more uniform when a mechanism design of mold core with chain shape was simulated. Additionally, the experimental results also revealed that the surface roughness significantly decreased from 1.8 μm Ra down to 0.28 μm Ra after 5 machining cycles, and calculating the percentage of improvement rate approximately 84% presented an excellent solution to reduce surface roughness. Furthermore, a novel mechanism with helical passageway was developed to perform multiple

flowing paths of abrasive medium, whose flowing behavior enhanced polishing effectiveness by increasing the abrasive surface area and radial shear forces [15-16]. The design of helical passageway was an effective solution to achieve the surface roughness uniformity of axial direction in polishing a circular hole. Based on above studies, present work will apply an optimal mold core with four helices to polish different polygon holes, which including square, hexagon and octagon holes are conducted to verify the polishing effects of different passageways in AFM. Motion behavior in multiple directions is evaluated when the abrasive medium in the passageways produces irregular variances in velocity and strain rate based on analytical results. Additionally, the measurements of different passageways are implemented to demonstrate the increase in the roughness improvement rate (RIR) and roughness uniformity for AFM process.

II. METHOD

A. Material Property

Generally, the behavior of abrasive medium during AFM can be considered as a non-Newtonian flow from a macro perspective, the power law is adopted to determine the relationships among viscosity, the shear rate and the temperature using CFD-ACE+ software. The following mathematical equation describes the material properties of an abrasive medium.

$$\mu = K\mu_0 e^{(a_1 T - a_2 T^2)} \dot{\gamma}^c \quad (1)$$

$$\text{where } c = n - 1 + a_3 \ln(\dot{\gamma}) + a_4 T \quad (2)$$

and μ = viscosity of abrasive medium

μ_0 = Zero shear rate viscosity

$\dot{\gamma}$ = Local calculated shear rate

n = Power law index

T = Local calculated temperature

K, a_1, a_2, a_3, a_4 = fluid properties of abrasive media.

Furthermore, a rheological device is used to determine the curve of shear rates relative to viscosities. Figure 1 shows the relationship curve between the viscosities and the shear rates for this medium. Finally, the material properties of viscosity can be calculated after substituting the coefficients in Table 1 into equations (1) and (2).

B. Experimental Procedure

In this study, Silicon carbon (SiC) is chosen as the abrasive material and mixed with the silicone gel uniformly. The weight concentration of the abrasive in the polymer gels is approximately 50 % and abrasive mesh of SiC is #100. In AFM process, a semi-solid polymer gel mixed in a typical proportion of abrasives is extruded by two hydraulic cylinders with a constant pressure to polish a work-piece surface. The extrusion pressure of hydraulic cylinder is 4.2 MPa and back pressure is around 2.1 MPa in this process. Figure 2(a) shows the diagram of AFM machining process. This investigation focuses on the uniform roughness of a radial distribution when polishing polygon holes. The maximum distance of a polygon work-piece is 16.0 mm and the axis length is 30.0 mm. Next, the polishing effectiveness of different passageways in a polygon hole is evaluated by designing different mold cores to study the motion of the

abrasive medium. Figure 2(b) shows the diagram for a helical core with approximately 15.0 mm diameter.

TABLE I
THE PROPERTY PARAMETERS OF A-SILICONE MATERIAL

K	μ_0	a_1	a_2	a_3	a_4	n
1	50000	0.026	0.0004	-0.1231	0.0716	1

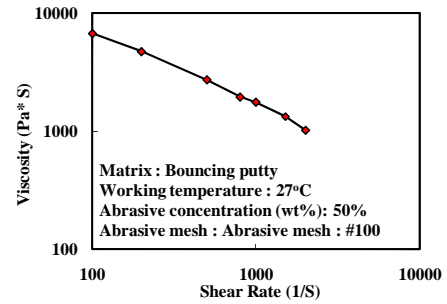
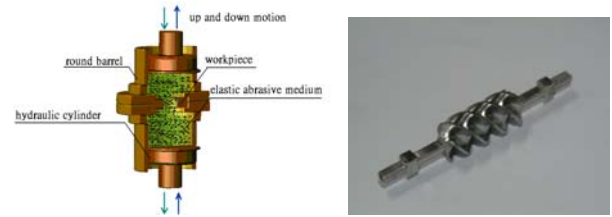


Fig. 1 Shear rates Effects on viscosities.



(a) Machining process of AFM

(b) A four helices core

Fig. 2 The diagrams of AFM and a four helices core.

III. RESULTS AND DISCUSSION

A. Simulation Results

This study has developed a numerical method to predict the flowing behaviours of the abrasive medium in polygon holes before a series of AFM-related experiments. Figure 3 shows the full modelling of mesh diagram of the abrasive medium without/with a four helices passageway. Simulation results for velocities and strain rates of the abrasive medium are used to determine how these different passageways affect the polishing precision during AFM.

1) *Effects of helical passageway on a square hole:* The subsection considers the motion of the abrasive medium without/with the mold core in polishing a square hole. Several mold cores with different helical shapes are developed to determine whether the flowing motion of an abrasive medium is altered. An optimal design of a four helices core is obtained based on simulated results. Figure 4 shows that the velocity curves of the square passageway without a mold core are almost zero for U and V directions, and only W direction has a regular curve of velocity. It demonstrates the abrasive medium retains a unitary axial motion. Next, Figure 5 indicates the velocity curve is almost zero only for U direction, both V and W directions have performed a regular curve of velocity; it reveals flowing motion of the square passageway with a four helices core is changed from unitary axial path to multiple axial paths. Furthermore, Figure 6 shows the axial curve diagram of strain rates in the square passageway without a mold core, and the upper and lower limit of strain rates is widely distributed from 2650 to 2250. Relatively, Figure 7 shows the axial curve diagram of strain rates in the square

passageway with a four helices core, and the upper and lower limit of strain rates is narrowly distributed from 690 to 530. Generally, the limit of strain rates being a bigger deviation from peak to peak will deteriorate the uniformity of surface roughness. On the other hand, the contour distributions of radial strain rates are given in Figure 8(a) and Figure 8(b). Figure 8(a) shows a widely range that the upper and lower limit of strain rates is distributed from around 2500 on edges to 700 on corner areas in the square passageway. Relatively, Figure 8(b) shows the radial curve diagram of strain rates in the square passageway with a four helices core, and the upper and lower limit of strain rates is narrowly distributed from 750 to 450. Calculating the percentage change of strain rates deviation can reduce from 72% to 40% for the square passageway. It also shows that the deviation of strain rates is distributed sharply on the entire radial surface, and the square passageway inserting with a helical core can improve the deviation percentage of strain rates approximately 32%. Therefore, this simulation results indeed indicate that the square passageway with a helical core predicts to enhance the uniformity precision of polishing.

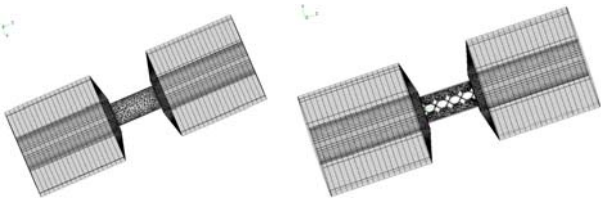


Fig. 3 CFD modelling diagram of the abrasive medium without/with a helical passageway.

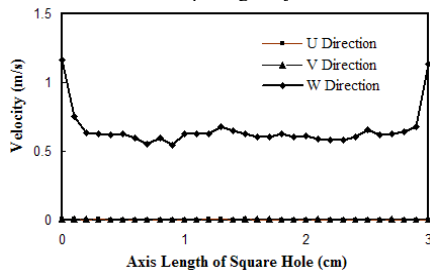


Fig. 4 The curve diagram of axial velocity in a square passageway.

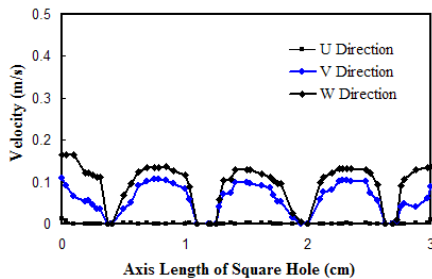


Fig. 5 The curve diagram of axial velocity in a four helices passageway.

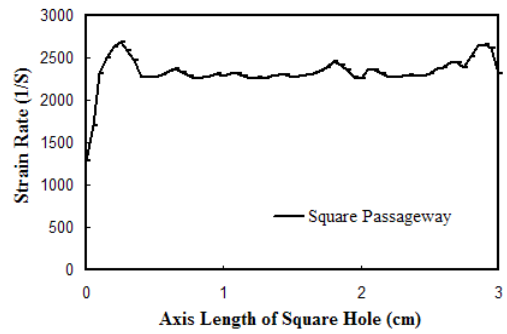


Fig. 6 The curve diagram of axial strain-rate in a square passageway.

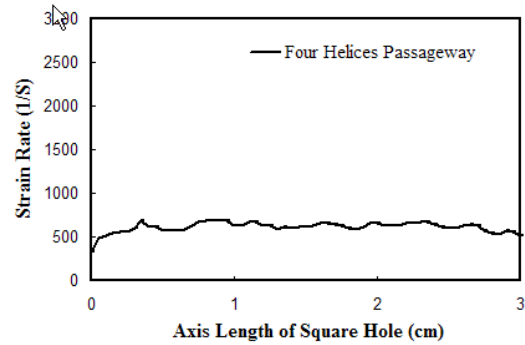
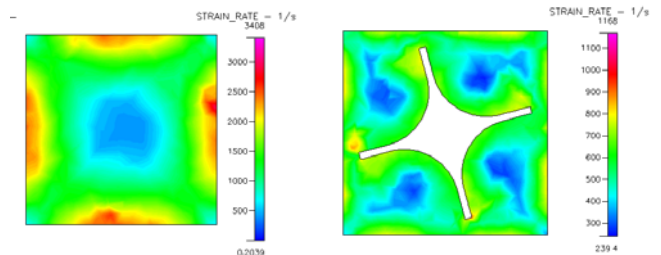


Fig. 7 The curve diagram of axial strain-rate in a four helices passageway.

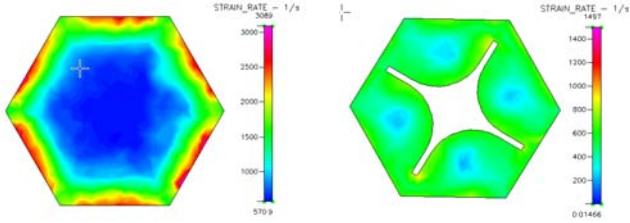


(a) Square hole without mold core (b) Square hole with four helices core

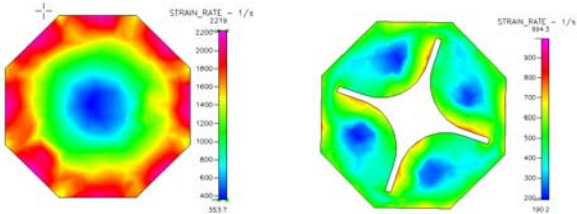
Fig. 8 The cross section diagram of radial strain-rate in square passageway.

2) *Effects of helical passageway on hexagon and octagon holes:* Different passageways in hexagon and octagon holes are conducted to verify the polishing effects of the abrasive medium in AFM. The simulation results of motion behaviour for axial velocities and strain rates are similar to the results of the square passageway. Thus, this study focus on the improvement rate of radial strain rates in radial direction of both hexagon and octagon passageways. Figure 9(a) shows that a widely range that the upper and lower limit of strain rates is distributed from around 2500 on edges to 1500 on corner areas in the hexagon passageway. Relatively, Figure 9(b) shows the radial curve diagram of strain rates in the hexagon passageway with a four helices core, and the upper and lower limit of strain rates is narrowly distributed from 800 to 600. Calculating the percentage change of strain rates deviation can reduce from 40% to 25% for the hexagon passageway. It shows that the hexagon passageway inserting with a helical core can improve the deviation percentage of strain rates around 15%. Similarly, Figure 10(a) shows that the upper and lower limit of strain rates is widely distributed from around 2000 on edges to 1300 on corner areas in the hexagon passageway. Relatively, Figure 10(b) shows the radial curve diagram of strain rates in the octagon passageway with a

four helices core, and the upper and lower limit of strain rates is narrowly distributed from 700 to 500. Calculating the percentage change of strain rates deviation can reduce from 35% to 29% for the octagon passageway. The improvement rate of helical passageway in octagon shape is obtained only approximately 6%. Therefore, this simulation results also indicate that hexagon and octagon passageways with a helical core predict to improve the uniformity precision of polishing.



(a) Hexagon hole without mold core (b) Hexagon hole with a helical core
Fig. 9 The cross section diagram of radial strain-rate in hexagon passageway.



(a) Octagon hole without a mold core (b) Octagon hole with a helical core
Fig. 10 The cross section diagram of radial strain-rates in octagon passageway.

B. Experimental Results

A batch samples of polygon holes of SKD-11 steel are cut out using WEDM process, in which the average surface roughness of polygon holes are approximately $1.8 \mu\text{m Ra}$ after machining. Next, polygon holes with different passageways can then be finished after the WEDM by using AFM. Generally, a series of experiments pick up ten positions in a sectional area to test the surface roughness after AFM. The RIR is defined as following equation (3) :

$$\text{RIR} = \frac{\text{SR}_{\text{origin}} - \text{SR}_{\text{polishing}}}{\text{SR}_{\text{origin}}} \quad (3)$$

where $\text{SR}_{\text{origin}}$ indicates the original surface roughness before AFM and $\text{SR}_{\text{polishing}}$ expresses the surface roughness after polishing. The roughness uniformity is defined for a surface roughness deviation between frontal side and middle side measurements. According to the simulation results, we adopt a four helices core with different polygon work-pieces to conduct a series of experiments. Experiment proceeding design a variety consists of different type and different size of mold cores to verify the effectiveness of helical passageway in AFM. Finally, an optimal design conditions including for four helices groove, 0.5 mm gap, 0.5 mm thickness of helical slot and one helical turn is obtained. The effects of surface polishing with a four helices passageway describe as follows :

1) Effects of helical passageway on surface roughness:

Figure 11 presents the polishing effects of the number of alternating cycles on surface roughness during AFM for 20 cycles in different passageways without a mold core. This figure displays that surface roughness decrease with

increasing in number of working cycles. Figure 12 shows the polishing results after 20 machining cycles for different passageways with a four helices core. According to the comparisons both Figure 11 and Figure 12, polygon passageways with a four helices core perform better efficiency than polygon passageways during polishing. The RIR is only 69.4% in the square passageway, but RIR reach 76.6% in the four helices passageway. Next, The RIR is 76.1% in the hexagon passageway, but RIR can reach 83.3% in a four helices passageway. Finally, the percentage change of RIR can improve from 78.9% to 86.1% for octagon passageway. Therefore, this study demonstrates the effectiveness of helical passageway for changing motion character from unitary axial motion to multiple axial motions, which obviously affects the average RIR in polygon holes AFM.

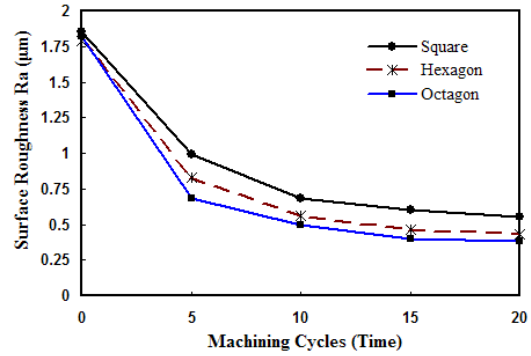


Fig. 11 The distribution diagram of surface roughness in different polygon passageway without a mold core.

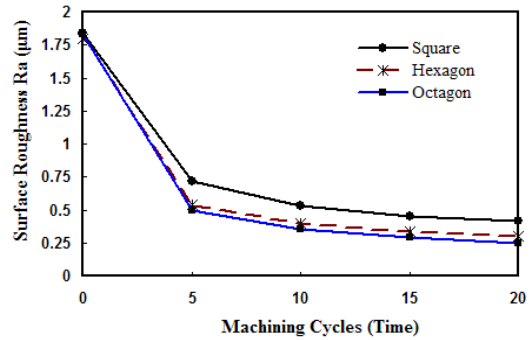


Fig. 12 The distribution diagram of surface roughness in different polygon passageway with a four helices core.

2) Effects of helical passageway on uniformity of surface roughness: In this investigation, frontal area and middle area of surface roughness measurement are implemented to verify the effects of uniformity of surface roughness after polygon holes polishing. Figure 13 shows the polishing results after 20 machining cycles for different measuring areas in the square passageways. According to the test results, it demonstrates the less change of a four helices passageway in surface roughness based on the measurement comparisons between frontal area and middle area. Thus, surface roughness is more uniform when a four helices core is utilized as finishing passageway. Similarly, the test results of both hexagon and octagon holes polishing are given in Figure 14 and Figure 15. They also reveal that abrasive medium in the polygon passageways with a four helices core can induce uniform polishing effect.

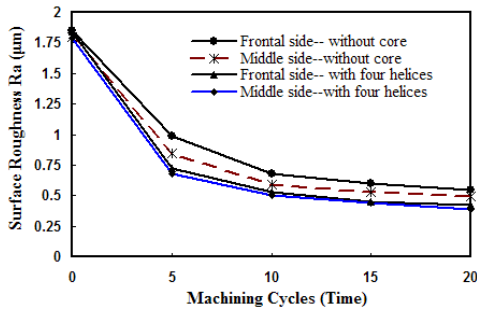


Fig. 13 The distribution diagram of surface roughness in square without/with four helices core.

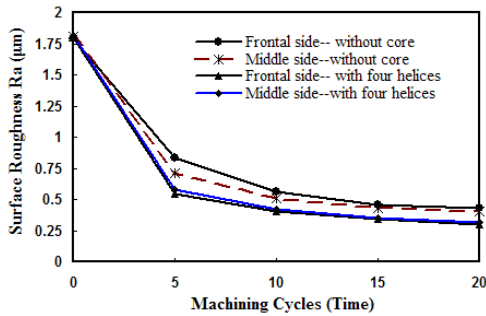


Fig. 14 The distribution diagram of surface roughness in hexagon without/with four helices core.

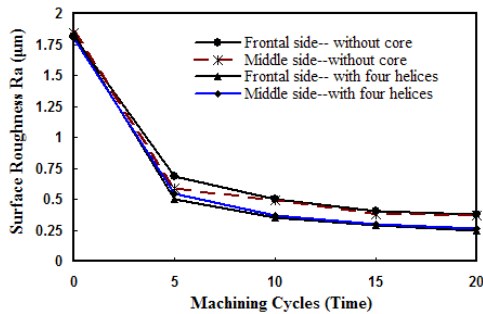


Fig. 14 The distribution diagram of surface roughness in octagon without/with four helices core.

IV. CONCLUSIONS

Based on the foregoing discussions in investigating the AFM polishing in polygon holes, the main conclusions are summarized as follows.

First, CFD-ACE⁺ numerical software is a suitable and effective simulation tool for demonstrating the optimum design of polygon passageways with a four helices core. The results show that the helical passageway creates flowing path from unitary axial motion to multiple axial motions to enhance the uniformity precision of polishing. Moreover, experimental results indicate that the polishing effectiveness of different passageways is consistent with analytical results. It reveals that polygon passageways with a four helices core perform better efficiency than only polygon passageways after 20 machining cycles. The RIR is only 69.4% in the square passageway, but RIR can reach 76.6% in the square passageway with a four helices core. Similarly, the percentage change of RIR can upgrade from 76.1% to 83.3% in the hexagon passageway with a four helices core. Next, the percentage change of RIR can improve from 78.9% to 86.1% for octagon passageway. For calculating all of the above comparisons, the percentage of

improvement rate all approximately 7% presents a good solution to reduce surface roughness. Finally, the results also demonstrate that surface roughness is more uniform when four helices core is utilized as finishing passageway. Therefore, helical passageway indeed creates significant efficiency on good surface roughness and uniformity in radial distributions for polishing polygon holes.

ACKNOWLEDGMENT

The authors would like to thank National Science Council of the Republic of China for financially supporting this research under Contract No. NSC 98-2221-E-231-007.

REFERENCES

- [1] A. C. Wang, B. H. Yan, X. T. Lee, F. Y. Huang, "Use of micro ultrasonic vibration lapping to enhance the precision of micro holes drilled by micro electro-discharge machining," *International Journal of Machine Tools and Manufacture*, 42 (2002) 915-923.
- [2] S. E. You, A. C. Wang, F. Y. Huang, B. H. Yan, "Precision improvement of micro slit by electro-chemical polishing," *Proceedings of the 17th National Conference on Mechanical Engineering*, 4 (2000) 73-80.
- [3] G. W. Chang, R. T. Hsu, B. H. Yan, R. H. Chang, "Study of applying magnetic abrasive finishing to improve EDM surface," *Proceedings of the 18th National Conference on Mechanical Engineering*, 4 (2001) 555-562.
- [4] B. H. Yan, Y. C. Lin, F. Y. Huang, "Surface modification of Al-Zn-Mg alloy by combined electrical discharge machining with ball burnish machining," *International Journal of Machine Tools and Manufacture*, 42 (2002) 925-934.
- [5] T. R. Loveless, R. E. Williams, K. P. Rajurkar, "A study of the effects of abrasive flow machining on various machined surfaces," *Journal of Materials Processing Technology*, 47 (1-2) (1994) 133-151.
- [6] L. J. Rhoades, "Abrasive flow machining-progress in productivity," *ASME Technical Paper*, MR 1993 (1993) 1-16.
- [7] V. K. Jain, S. G. Adsul, "Experimental investigations into abrasive flow machining (AFM)," *International Journal of Machining Tools & Manufacture*, 40 (7) (2000) 1003-1021.
- [8] V. K. Jain, C. Ranganatha, K. Muralidhar, "Evaluation of rheological properties of medium for AFM process," *Machine Science and Technology*, 5 (2) (2001) 151-170.
- [9] R. K. Jain, V. K. Jain, P. M. Dixit, "Modeling of material removal and surface roughness in abrasive flow machining process," *International Journal of Machine Tools and Manufacture*, 39 (12) (1999) 1903-1923.
- [10] R. K. Jain, V. K. Jain, "Finite element simulation of abrasive flow machining," *Proceedings of the Institution of Mechanical Engineers -- Part B -- Engineering Manufacture*, 217 (12) (2003) 1723-1736.
- [11] R. K. Jain, V. K. Jain, "Stochastic simulation of active grain density in abrasive flow machining," *Journal of Materials Processing Technology*, 152 (1) (2004) 17-22.
- [12] A. C. Wang, C. H. Liu, K. Z. Liang, S. H. Pai, "Study of the rheological properties and the finishing behavior of abrasive gels in abrasive flow machining," *Journal of Mechanical Science and Technology*, 21 (2007) 1593-1598.
- [13] A. C. Wang, L. Tsai, K. Z. Liang, C. H. Liu, S. H. Weng, "Uniform surface polished method of complex holes in abrasive flow machining," *Transactions of Nonferrous Metals Society of China*, Vol. 19 (2009) 250.
- [14] A. C. Wang, S. H. Weng, "Developing the polymer abrasive gels in AFM process," *Journal of Materials Processing Technology*, 192-193 (2007) 486-490.
- [15] A. C. Wang, K. Y. Chen, K. C. Cheng, H. H. Chiu, "Elucidating the effects of helical passageway in Abrasive Flow Machining," *Advanced Materials Research*, 264-265 (2011) 1862-1867.
- [16] K. Y. Chen, K. C. Cheng, A. C. Wang, Y. C. Lin, "Study the rheological properties of abrasive gel with various passageways in Abrasive Flow Machining," *Advanced Materials Research*, 126-128 (2010) 447-456.